

Appendix B: Experimental Procedures and Results

This appendix focuses on the experimental procedures and equipment used to study fluidization characteristics during salt loading experiments. Two different fluidized beds were used to complete the experiments. The first fluidized bed was made out of alumina and designed by Pete Czerpak (M.S. 1998) to study alumina and silica particles in the 100-250 micron size range. A brief description of this first generation system is given below. The second generation fluidized bed was made out of Inconel™, and designed to uniformly fluidize 500-micron silica glass ballotini.

The primary component used in both the generation I and II systems is a Thermal Technology Astro laboratory furnace designed to provide a 0.46 m (1.51 ft) hot zone with a 0.11 m (4.3") internal diameter (ID). The furnace itself is capable of reaching temperatures upward of 2300°C (4772°F). A Eurotherm Controls EPC Controller controls the furnace element temperature. The temperature is measured with a pneumatically controlled retractable thermocouple up to 1100°C (2012°F) and then a dual wavelength optical pyrometer measures temperatures higher than 1100°C (2012°F). A Honeywell Limit Control Module monitors the maximum temperature allowable for the equipment and can affect process shutdown. The reactor is cooled using house water at a flow rate greater than 17 Lpm (4.5 gpm). The graphite element is isolated from the centerline of the furnace with a 9.21 cm (3.625") ID alumina muffle tube.

B.1) Generation I Process Description

The Generation I process schematic is given in Figure B.1. The Generation I Process used an alumina fluidized bed reactor made by Coors Ceramic Co. The fluidized bed consisted of two alumina tubes approximately 6.79 cm (2.675") ID and extended the length of the furnace's hot zone. The distributor plate was made out of 0.3 cm (.11") thick alumina with 18-0.01 cm (0.039") holes. Peter Czerpak completed the distributor plate design and Coors Ceramic Co made the distributor plate.(Czerpak 1998). A schematic for the fluidized bed is shown in Figure B.2. The distributor plate was permanently secured between the two alumina reactor tubes with a larger diameter alumina coupling tube and Aremco Ceramabound 503 ceramic cement. Nitrogen acted as the fluidizing gas and the inert sweep gas to protect the graphite element. Nitrogen was supplied from a large liquid nitrogen dewer. If the large dewer's pressure dropped below 2.76E5 Pa (40 psig), nitrogen from a high-pressure gaseous nitrogen cylinder began flowing. Three Brooks Flowmeters with varying capacities controlled the flow of nitrogen to the fluidized bed. Two Dwyer flowmeters delivered sweep gas to the element chamber and sight glass windows.

All gas supplied to the furnace and fluidized bed was vented to the laboratory hood via 0.635 cm (0.25") stainless steel tubing to accommodate the high temperature gases from the fluidized bed. The nitrogen was filtered by a microfilter (Balston Model 82-700-BX) to remove any fine particles prior to entering the flowmeters. The process gas was also filtered after leaving the fluidized bed. The fine particles were removed to prevent clogging in the 0.635 cm (0.25") stainless tubing on the way to the hood.

Generation I Process and Sweep Gas Flow Diagram

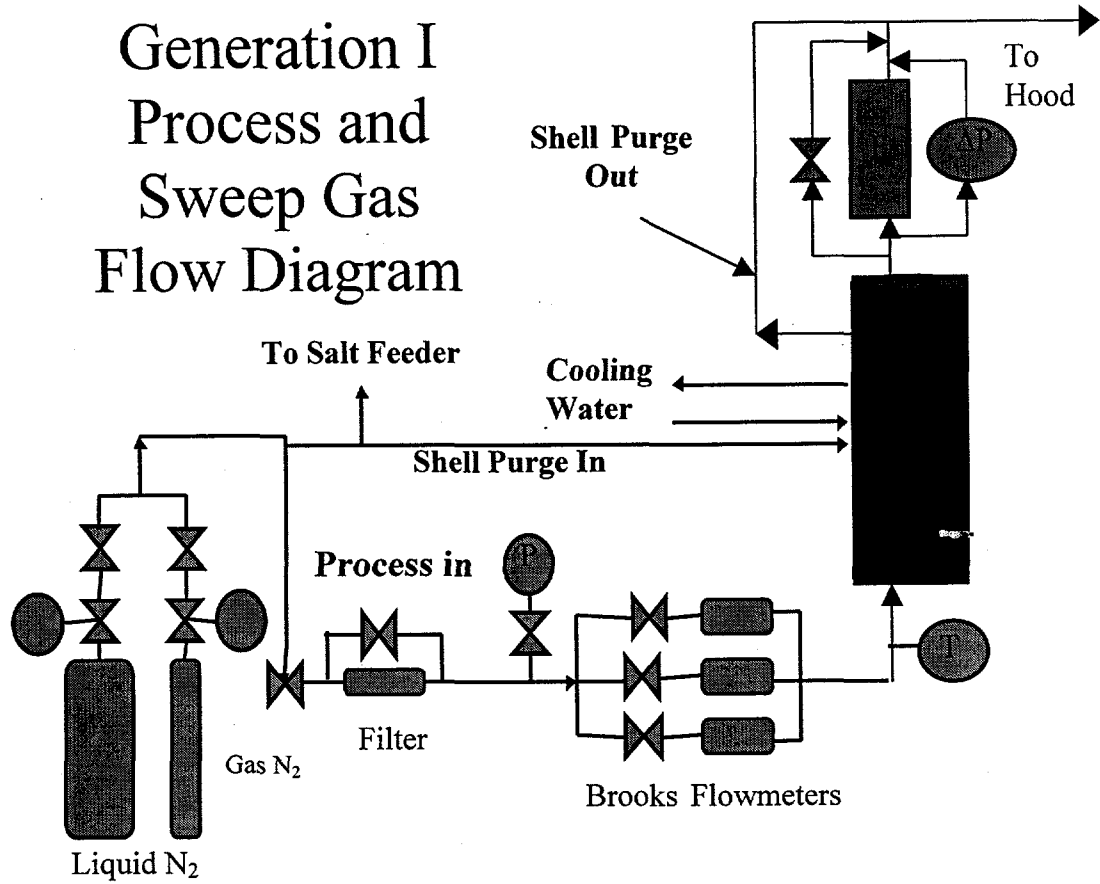


Figure B.1 Generation I Process and Sweep Gas Flow Diagram.

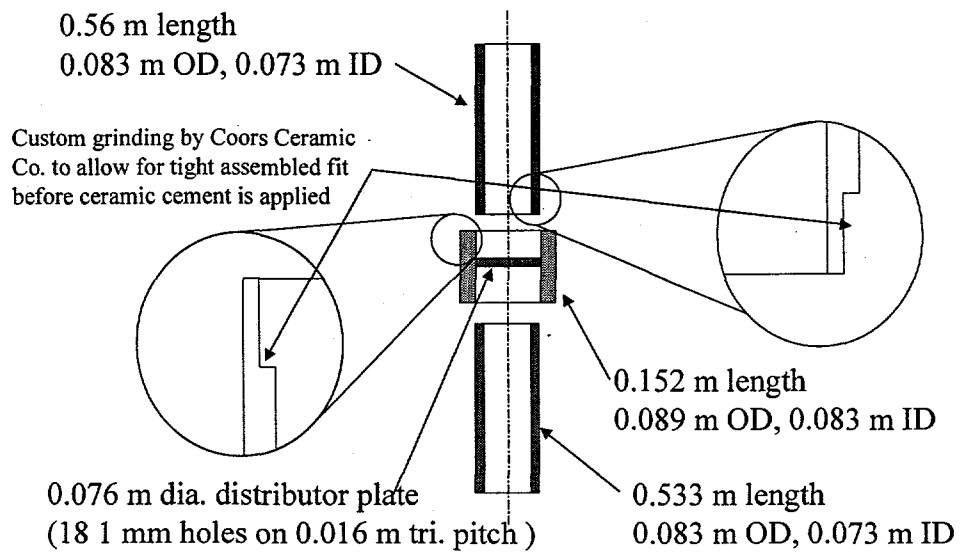


Figure B.2 Generation I Fluidized Bed Reactor Schematic.

The temperature in the bed was measured with an Omega Sciences type K, ungrounded, Inconel™ sheathed, closed-tip thermocouple. The thermocouple enters the reactor through a Swagelock® 0.635 cm (0.25") tube fitting connection located in the top furnace plate and extended down into the fluidized bed, position just above the distributor plate. The temperature of the gas entering the fluidized bed was measured along with the inlet pressure for use in calculating the correct volumetric flow rate. The inlet pressure was measured using another Validyne DP-15 pressure transducer. The volumetric flow rate and superficial velocity through the fluidized bed were calculated.

The pressure drop across the fluidized bed is the critical measurement for understanding the particles' fluidization characteristics. The ΔP was measured by first inserting an uncapped 0.635 cm (0.25") stainless steel tube through the top reactor plate to the bottom of the particle. The pressure above the bed was measured with an uncapped, 0.32 cm (0.125") stainless steel tube, which also passed through the top reactor plate. The tube opening for the low-pressure measurement is located at the top of the fluidized bed reactor as seen in Figure B.3. Considering the importance of the pressure drop measurement, two different measuring devices were used to determine the pressure drop. A Validyne DP-15 pressure transducer (PTDR# 1) was used in conjunction with a Dwyer Magnehelic 0-2.5E3 Pa (0-10" of H₂O) low pressure gauge. The gauge pressure in the reactor above the distributor plate was measured with a Dwyer Magnehelic 0-1.25E4 Pa (0-50" of H₂O) low pressure gauge.

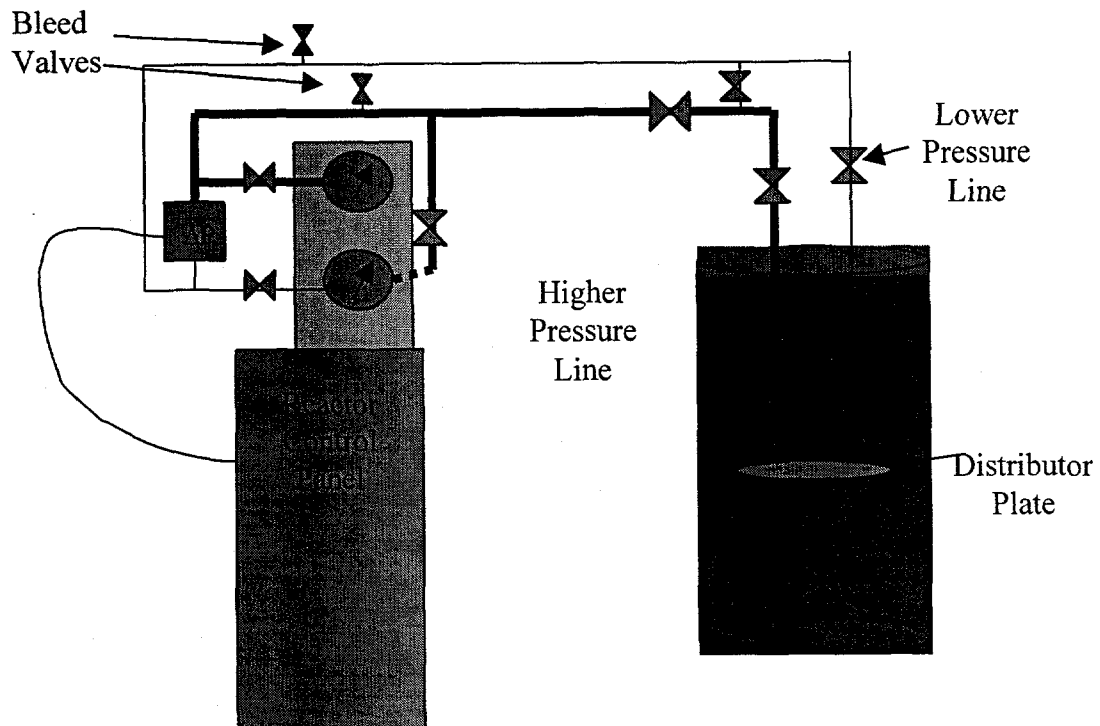
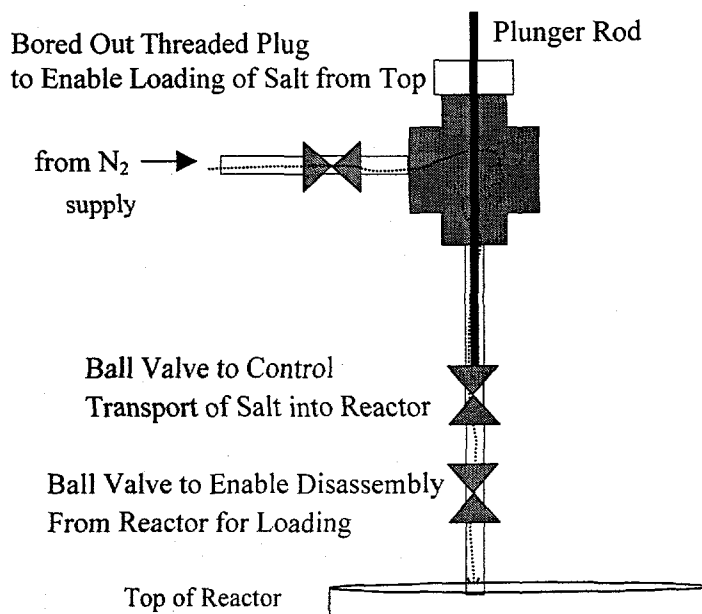


Figure B.3 Generation I Pressure Drop Measuring System.
 Figure B.4 Salt Injector Schematic.



The salt was injected into the fluidized bed reactor through the top reactor plate. The pneumatic salt feeder seen in Figure B.4 used compressed N₂ from the gaseous N₂ cylinder. When the salt feeder was in use the gaseous N₂ tank was isolated from the process flow nitrogen to prevent disrupting the flow through the fluidized bed reactor. The salt feeder was connected to the gaseous nitrogen line with flexible stainless steel tubing. The plunger rod was made from an old coat hanger and inserted into the feeder through a 0.32 cm (0.125") Swagelock® tube fitting. The feeder itself is 0.95cm (0.375") stainless steel tubing with two Swagelock® ball valves. The 0.95 cm (0.375") tubing enters the reactor through another Swagelock® tube fitting. The salt feeder extends down into the reactor where the salt is released approximately 1.5 cm (6") above the surface of the bed.

B.2) Generation II Process Description

A number of changes were made to the Generation I set up to accommodate larger particle sizes. A new fluidized bed reactor was designed out of an 8.9 cm (3.5") O.D. Inconel™ tube. In the Generation II system, compressed air is used as the fluidizing gas. Figure B.5 shows the new process and sweep gas flow schematic. There are a number of changes that deserve mentioning.

First, a fourth Brooks Flowmeter was installed to handle the larger volumetric flow rates of gas needed to fluidize larger particles. The piping from the house compressed air line is 0.635 cm (0.25") galvanized steel with a series of brass 0.635 cm (0.25") ball valves to control the flow. A regulator controls the compressed air's pressure, which is typically set between 4.46-4.84E5 Pa (65-70 psig). The compressed air flows through Parker coalescing and adsorbing filters, each with an auto drain. The gas' pressure is still measured after leaving the flowmeters with a Validyne DP-15 pressure transducer referred to as PTDR #2. The air leaving the flowmeter enters 0.635 cm (0.25") galvanized steel tubing before entering 0.6 m (2') of 1.59 cm (0.675") I.D. Tygon tubing which is attached to the furnace bottom plate with a hose clamp and tubing nipple. Thin walled 1.25 cm (0.5") O.D. stainless steel tubing transports the post reactor gas to the hood. A Filterite porous metal filter made by the Memtec of America Corporation filters the compressed air on the way to the hood. Another Validyne pressure transducer measures the pressure drop across the filter. This pressure transducer is referred to as PTDR #3.

The Inconel™ fluidized bed reactor is 114.3 cm (43") long with a 7.62 cm (3.0") ID. The distributor plate is made out of 304 Stainless Steel, and has a 7.87 cm (3.1") diameter and 0.127 cm (0.05") thickness. The distributor plate was welded into the Inconel™. The distributor plate has approximately 70 holes, each 0.05 cm (0.020") in diameter, arranged in a 0.8 cm (0.32) triangular pitch pattern.

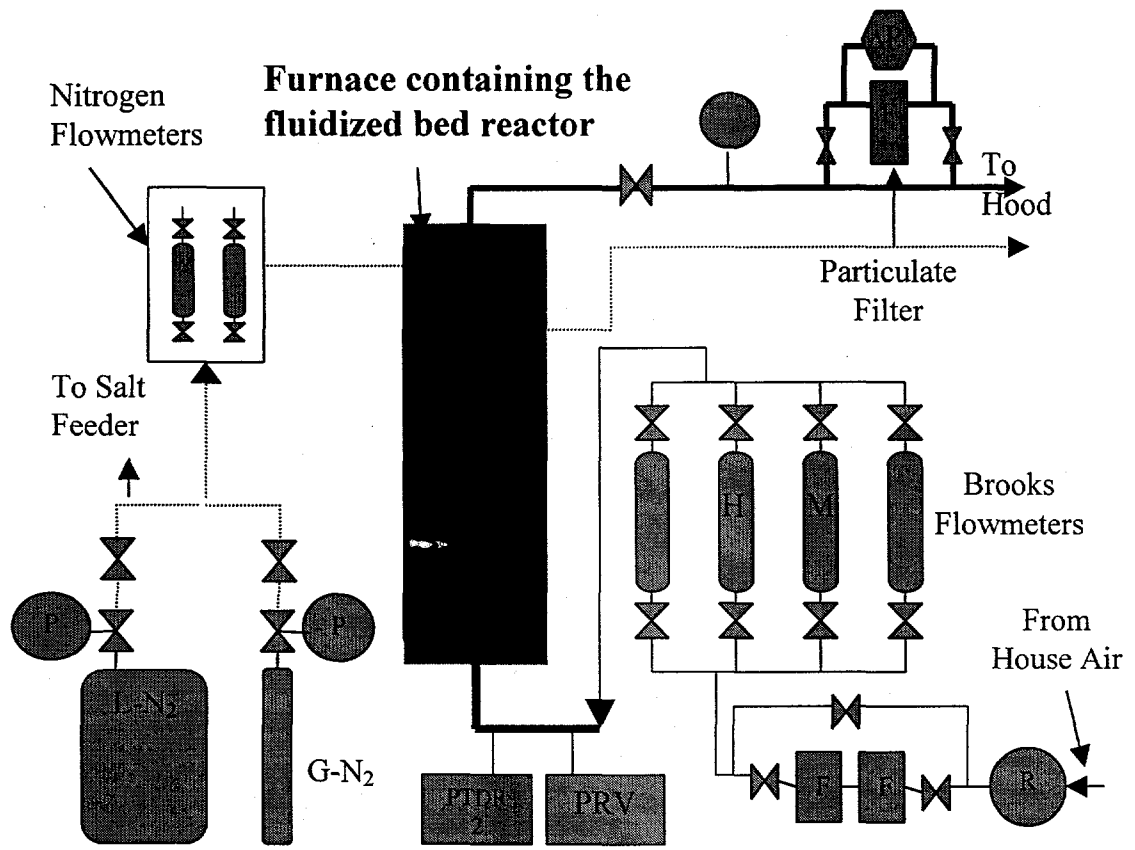


Figure B.5 Generation II Process and Sweep Gas Flow Diagram.

The inert sweep gas is still nitrogen and is supplied from the same source previously mentioned for the Generation I system. There are three main differences in the piping set up for the nitrogen. All of these changes were made to reduce the risk of compressed air entering the graphite element chamber. First, the 0.635 cm (0.25") stainless steel tubing that connected the sweep and process flow in the Generation I setup was removed and capped in order to completely separate the compressed air lines from the nitrogen lines. Next, the sweep gas was given its own vent line to the hood made out the 0.635 cm (0.25") stainless steel. Finally, the Tygon tubing line that carried nitrogen to the top plate reactor sight window was removed and capped. Removing this line prevented the compressed air flowing through the fluidized bed from flowing back through the nitrogen line and contaminating the graphite element chamber.

A couple of changes were made to the pressure drop measuring system as seen in Figure B.6. Two in-line filters were installed to prevent the support from traveling up the stainless steel tubing and contaminating the pressure transducer (PTDR#1) and pressure gauges. This is only an issue if a valve happens to be turned the wrong way at an in-opportune moment. An additional, 0.635 (0.25") stainless steel tube was inserted through the bottom reactor plate for a number of reasons. The additional tube, which opens a couple of centimeters below the distributor plate, measures the pressure of the gas entering the reactor. The stainless steel tube that measures the pressure above the distributor plate was capped and 12-1 mm holes were drilled equidistant around the outer circumference to reduce clogging.

The final set of experiments used a different method for introducing the salt into the fluidized bed reactor. The method used water as the vehicle for salt transport into the reactor. The aqueous salt solution was injected from a syringe through 0.32 cm (0.125") stainless steel tubing down into the reactor. The water would flash-off and the salt would in theory be left in an even coating on the particles. See Figure B.7 for a schematic.

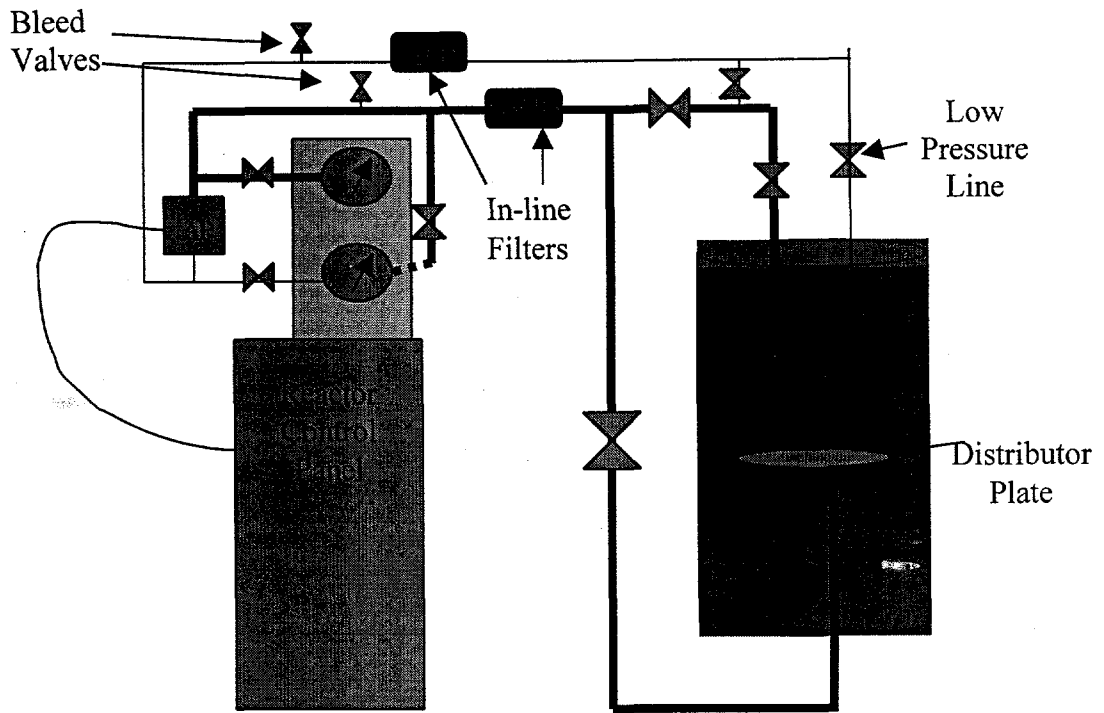
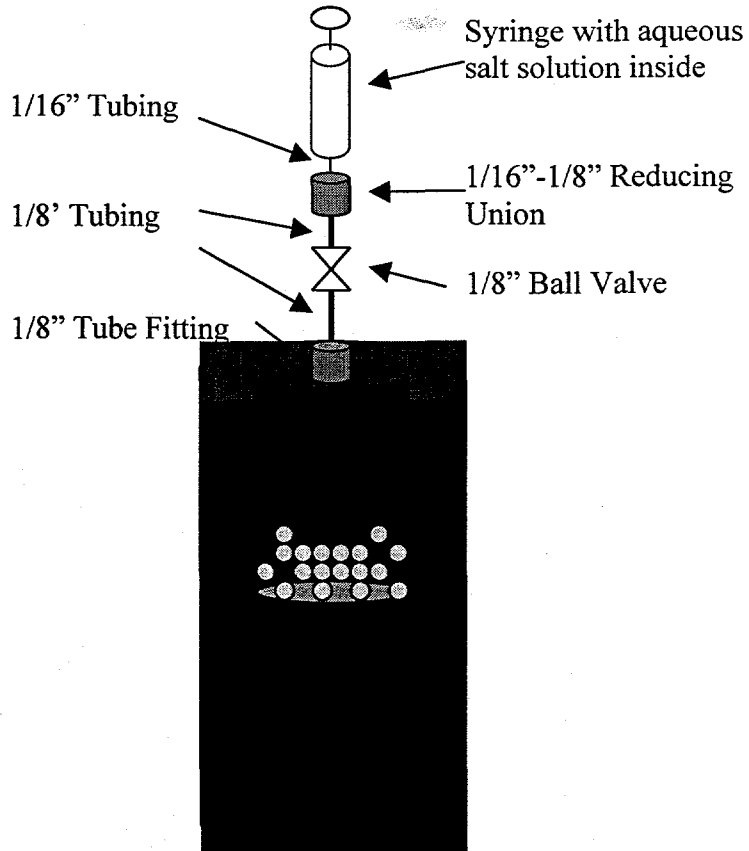


Figure B.6 Generation II Pressure Drop Measurement.

Figure B.7 Aqueous Salt Injection System.



B.3) Generation I Data Collection Procedures/Results

In this section, two supports were tested to ascertain their salt loading capability. The two supports explored were U.S. Silica F-110 and L-60 whose important characteristics are listed in Table B.1. One goal centered on achieving complete fluidization of the support material. In previous experiments completed using these supports, the pressure drop measured for a bed mass of 350 gm and a reactor diameter of 6.8 cm (2.675") was consistently 30-40% below the theoretical ΔP . The theoretical value for a pressure drop across a fluidized bed at the point of minimum fluidization is calculated by dividing the weight of the support material by the cross sectional area of the reactor tube (Kunii and Levenspiel 1991). The theoretical pressure drop for these supports should have been 897 Pa (3.6 inches of H₂O) based on this postulate. Presumably, the lower pressure drop across the bed of particles was caused by incomplete fluidization of the support particles.

A Dwyer Magnehelic Gauge (0-2.49E3) Pa ((0-10)" of H₂O) was used in conjunction with the Validyne pressure transducer (PTDR#1) to provide additional confidence that the measurements were accurate.

Table B.1 Support Material Properties.

Designation	Supplier	Avg d_p (μm)	Loose Bulk Density (gm/cm^3)
F-110	US Silica	110	1.55
L-60	US Silica	227	1.48

The method in which the pressure drop measurement was determined is different from previous experiments for the Generation I fluidized bed. Previous experiments measured the nitrogen's pressure prior to entering the furnace and then after it left the furnace. Figure B.8 shows how this was accomplished. In order to use this method, the pressure drop across the distributor plate, as a function of the gas flow rate and temperature, must be determined. In addition to that correction, the pressure drop across the large 5 mm alumina particles also needs to be known as a function of the gas flow rate and temperature. The 5 mm alumina particles just mentioned prevented the much smaller support particles from falling through the distributor plate and aided in uniformly distributing the gas flow through the fluidized particles. The pressure drop across the bed of fluidized particles is easily determined if these two quantities are known. The problem with using this method is that there is an error associated with each measurement taken to obtain the pressure drop across the distributor plate and the bed of stationary particles. Measuring the pressure drop from the bottom of the fluidized particles and then at some height above the bed is a preferred method. This method was adopted for Generation II and I experiments. A visual schematic for this method is found in Figures B.3 and B.5.

B.3a) Minimum Fluidization Curve Procedure

Approximately 500 gm of the 5 mm Al_2O_3 spheres were initially loaded into the fluidized bed reactor through the top slight glass window. Nitrogen flow was initiated through the bed to prevent the smaller material from falling down through the large particles. Next 350 grams of the designated support material was loaded into the bed. In order to understand the molten salt's affect on the interparticle forces between the particles, a baseline for a system where the interparticle forces are assumed to be negligible was established. This is one of the reasons minimum fluidization curves for the various support materials were determined prior to adding salt to the bed

To obtain the minimum fluidization curves, the volumetric flow was increased to well above the minimum fluidization point. The velocity at which the pressure drop no longer substantially increases with increased flow rate signifies the minimum fluidization point (Kunii and Levenspiel 1991). The flow rate was slowly decreased and the pressure drop readings from both pressure transducers and pressure gauges were recorded along with the corresponding flow rate. The flow rate was decreased well past the point of minimum fluidization, but care was taken not to decrease the flow to the point that the particles began to fall through the distributor plate. The flow rate was then increased to see if a specific flow rate produces the same pressure drop. Initially, runs were completed to obtain the minimum fluidization curve for F-110 with the large Al_2O_3 spheres present below the smaller silica particles. This experiment's results are found in Figure B.9. It was extremely difficult to determine where the minimum fluidization point is on the figure due the consistent increase in the pressure drop with flow rate, but it most likely resides between (1.0-1.75) cm/s. It was suspected that the problem with the pressure drop increasing above the minimum fluidization point might involve the silica support getting trapped in the alumina packed bed. By increasing the flow rate, more and more, of the silica particles left the bed, causing the pressure drop to increase. Figure B.10 shows the result of a

minimum fluidization experiment for the same particles at ambient temperature where no alumina buffer support was used.

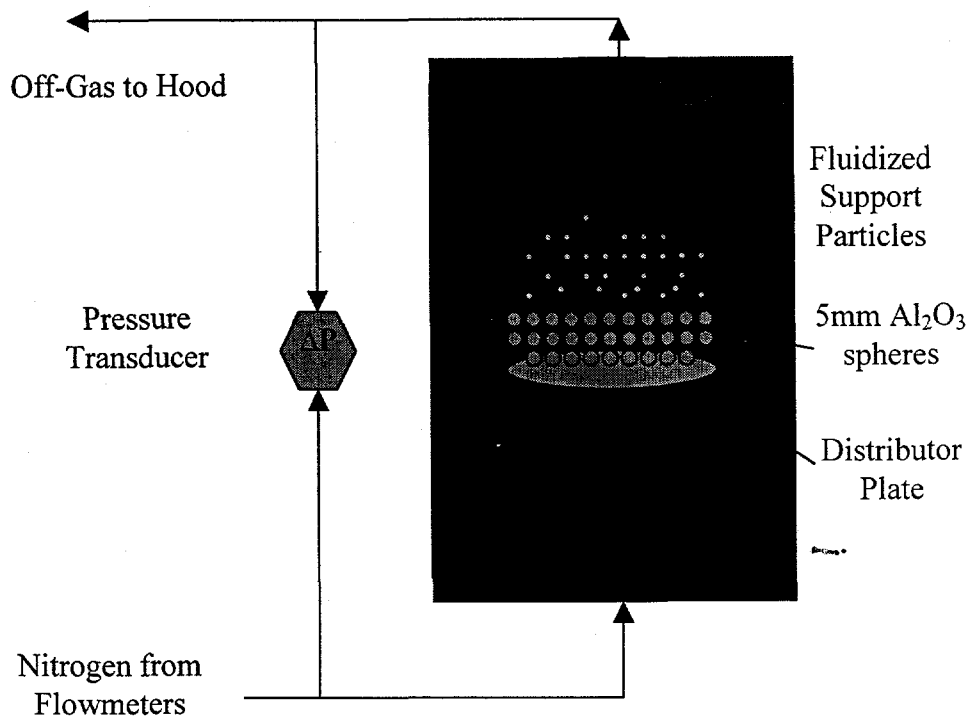


Figure B.8 Schematic for an Alternate Method for Calculating the Pressure Drop Across the Fluidized Bed.

Minimum Fluidization Curve: Pressure Drop vs Superficial Velocity (Temp 25°C, Support 350 gm of US Silica F-110, with 500 gm Al₂O₃ Buffer Support)

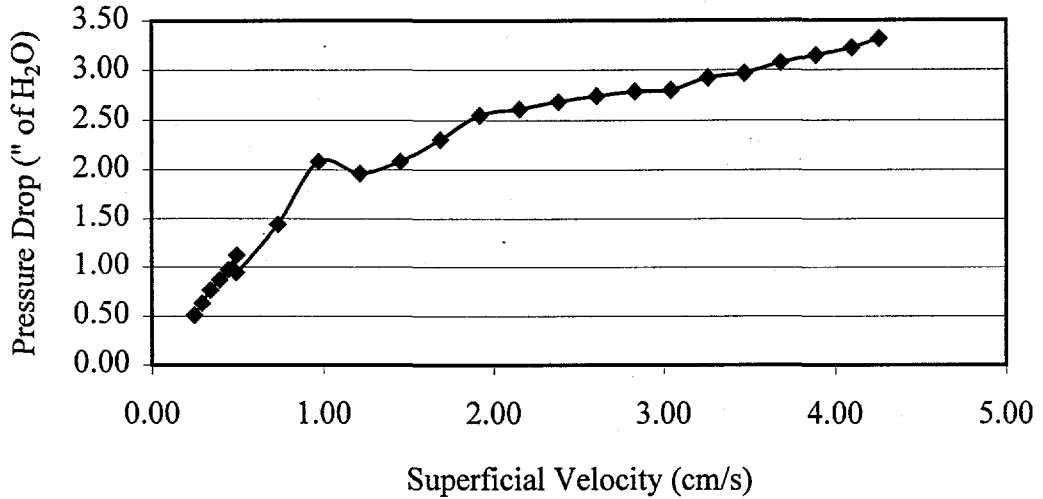


Figure B.9 Minimum Fluidization Curve for 350 grams of US Silica F-110 at 25°C with Buffer Support.

Minimum Fluidization Curve: Pressure Drop vs Superficial Velocity (Temp 25°C, Support 350 gm US Silica F-110, No Buffer Support)

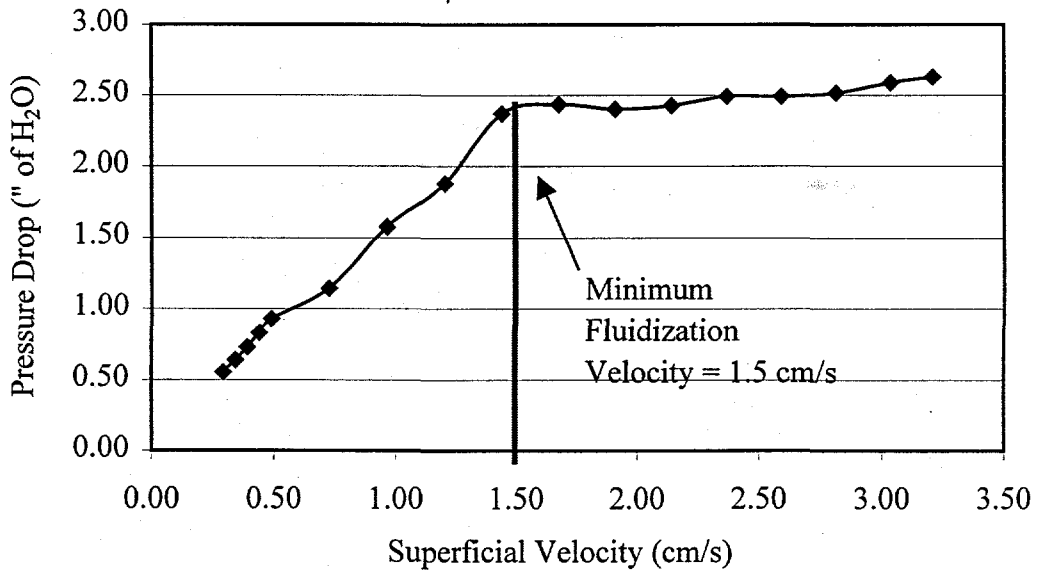


Figure B.10 Minimum Fluidization Curve for 350 grams of US Silica F-110 at 25°C with no Buffer Support.

The minimum fluidization point is in the neighborhood of 1.5 cm/s and the pressure drop beyond that point is fairly constant. The curve looks like a classical fluidization curve for this type of particles, except the pressure drop is much lower than the theoretical value of 897 Pa (3.6" of H₂O). In order to check the accuracy of the two pressure measuring devices, a U-tube manometer was constructed and attached to the bleed valves seen in Figure B.3. The manometer pressure drop measurement typically fell between the other two experimental readings. After visually observing the fluidization characteristics of the bed at ambient temperature, it appeared that bubbling only occurred in one region of the bed.

The inability to completely fluidize the particles was a problem that could not be corrected without designing a new distributor plate. Unfortunately, due to the nature of alumina, in house changes to the fluidized bed reactor were impossible. As the Generation II reactor was designed and built, further experiments with the F-110 and L-60 were conducted. Prior to conducting the salt loading experiments, the minimum fluidization curves for F-110 and L-60 at elevated temperatures were obtained. The temperature region of interest was between 300-500°C because of the melting point and thermal stability of the salt used for salt loading experiments. The salt, LiNO₃, melts at 251°C and dissociates at 600°C. The fluidization curves for the F-110 support particles at 300°C and 400 °C are shown in Figures B.11 and B.12. Figure B.13 shows the minimum fluidization curve for the L-60 support at 500°C. The minimum fluidization velocities for each curve are 0.85 cm/s, 0.8 cm/s, and 2.9 cm/s respectively.

Minimum Fluidization Curve: Pressure Drop vs Superficial Velocity (Temp - 300oC, Support 350 gm of US Silica F-110, No Buffer support)

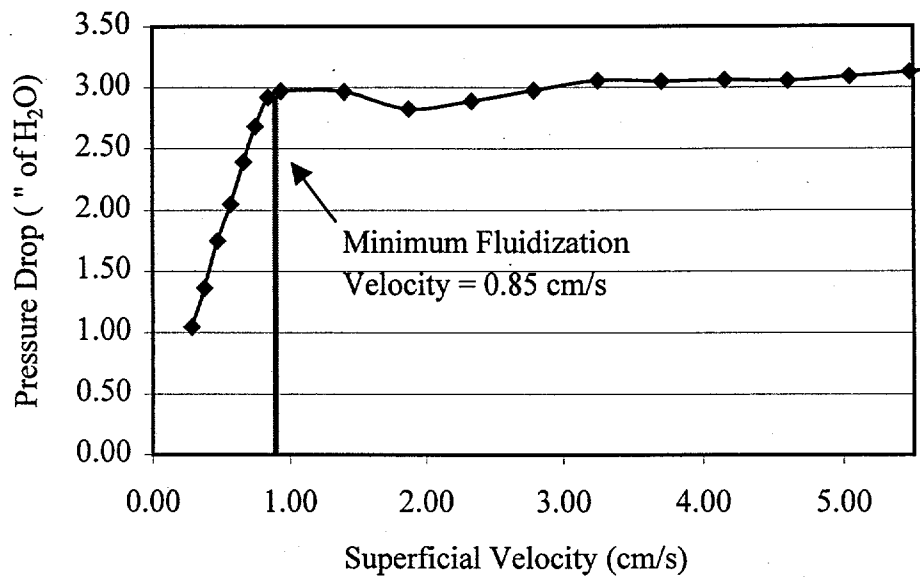


Figure B.11 Minimum Fluidization Curve for 350 grams of US Silica F-110 at 300°C.

Minimum Fluidization Curve: Pressure Drop vs Superficial Velocity (Temp - 400oC, Support 350 gm of US Silica F-110, No Buffer support)

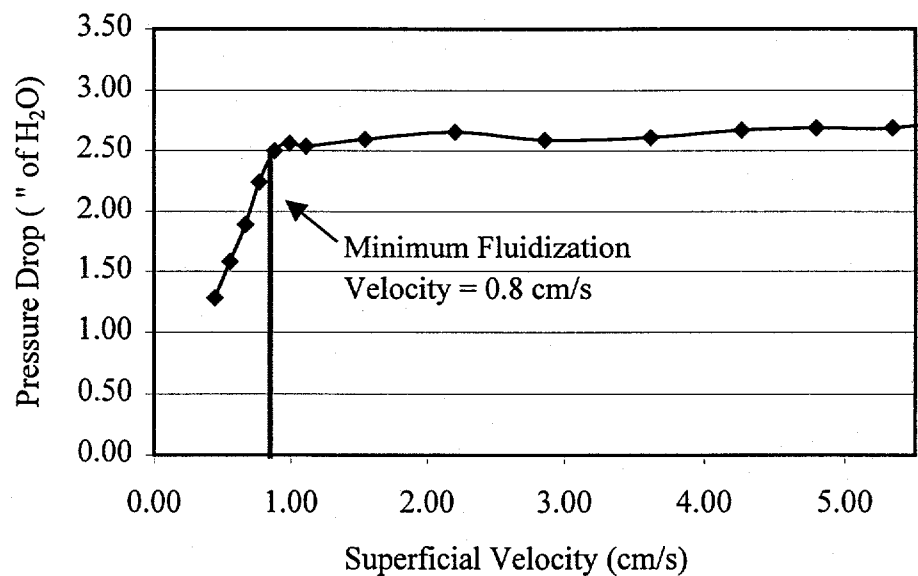


Figure B.12 Minimum Fluidization Curve for 350 grams of US Silica F-110 at 400°C.

Minimum Fluidization Curve: Pressure Drop vs Superficial Velocity (Temp - 500oC, Support 350 grams of US Silica L-60, No Buffer Support)

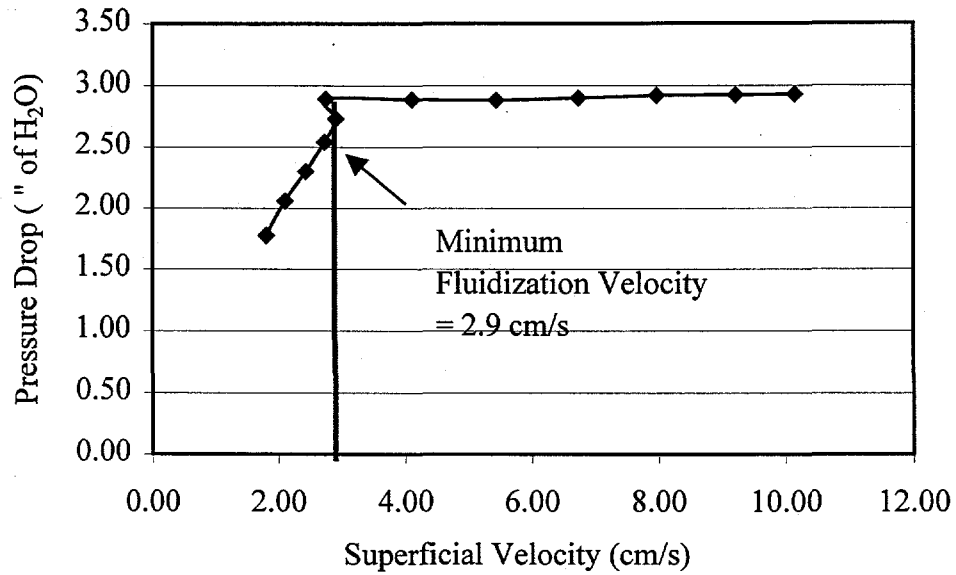


Figure B.13 Minimum Fluidization Curve for 350 grams of US Silica L-60 at 500°C.

For a sanity check, the L-60 minimum fluidization curve at ambient temperature was determined experimentally. The theoretical minimum fluidization velocity for silica particles with a sphericity of 0.9 and an average particle diameter of 250 microns was calculated. The u_{mf} theoretical was 4.97 cm/s just slightly larger than the experimentally determined value for the smaller L-60 particles of 4.8 cm/s. The close proximity of the theoretical and experimental minimum fluidization values provided confidence that the flowmeters and the procedure used to calculate the superficial velocity were sound.

For an undetermined reason, the pressure drops measured above the minimum fluidization point were different for all three cases. During the process of running the experiments, the U-tube manometer readings were compared to the pressure drop values given by the pressure transducer and pressure gauge. Again, the manometer's readings closely matched those given by the pressure transducer and pressure gauge.

B.3b) Salt Loading Experiments.

Figures B.14-B.16 contain the pressure drop across the bed of particles as a function of salt loading. The salt loading experiments were run at three different temperatures, different multiples of minimum fluidization velocity, and with two different size supports. By varying these parameters, one could begin to understand how the dimensionless groups important in the force balance between the particles affected the salt loading capability under different physical conditions.

The salt was added to the reactor using the pneumatic salt feeder in 1 gram increments. The pressure drop readings were recorded typically 20-30 minutes after the system had presumably reached a steady state. From Figures B.14-B.16, a clear trend does not exist between any of the cases. The data were also not consistent with the results obtained by Czerpak (Czerpak 1998). Figure B.14 shows the most promising results with a gradual pressure drop increase during the addition of the first seven grams of salt followed by an apparent collapse. Unfortunately, it was not made a practice to increase the flow rate through the bed to witness how that affected the pressure drop. Presumably, if the pressure drop remained constant even while increasing the flow rate, the bed was still in a fluidized state. This procedure was adopted for the Generation II experiments. The validity of the pressure drop readings were questionable due to the fact the pressure tube that measured the pressure directly above the distributor plate was typically clogged with particles and salt. Changes in the pressure drop measuring system were made to alleviate this problem for the Generation II experiments.

Figure B.14 Salt Loading Experiment with LiNO_3 for 350 grams of US Silica F-110 at 300°C.

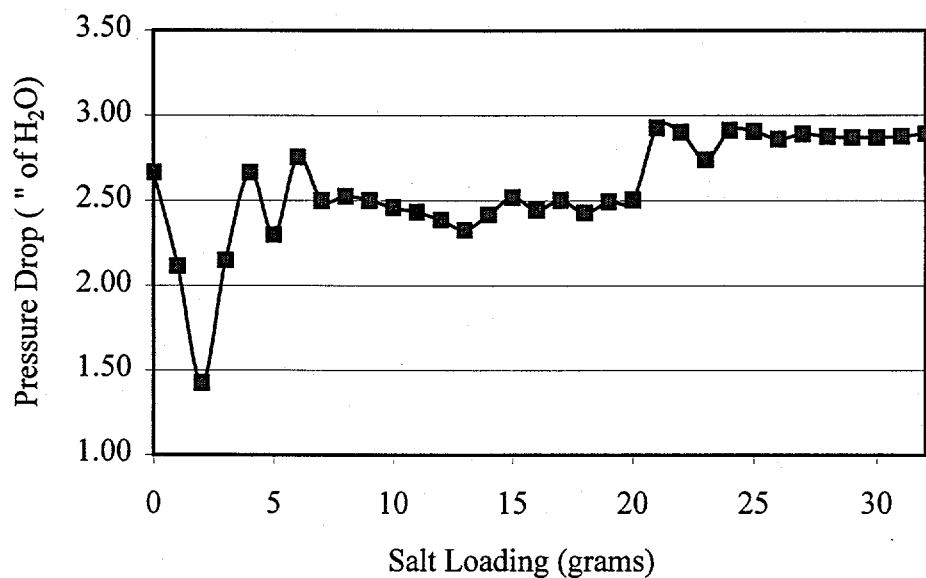
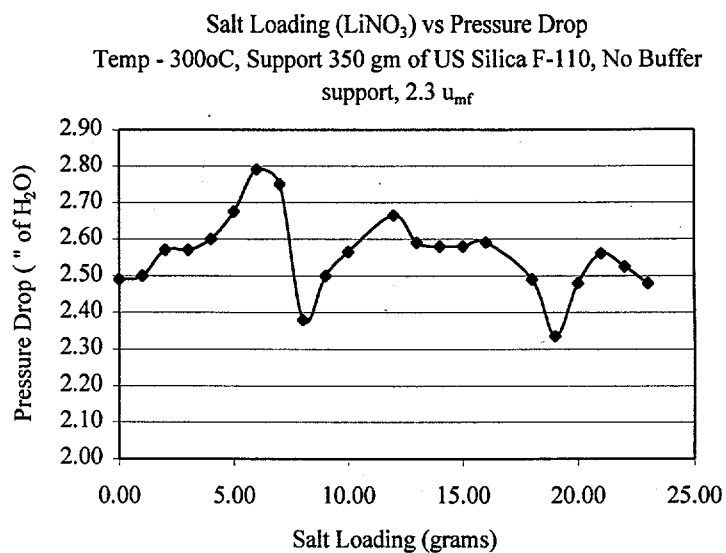


Figure B.15 Salt Loading Experiment with LiNO_3 for 350 grams of US Silica F-110 at 400°C.

Salt Loading (LiNO_3) vs Pressure Drop
(Temp- 500oC, Support 350 gm of US Silica L-60, No Buffer
Support, $3\mu\text{m}$)

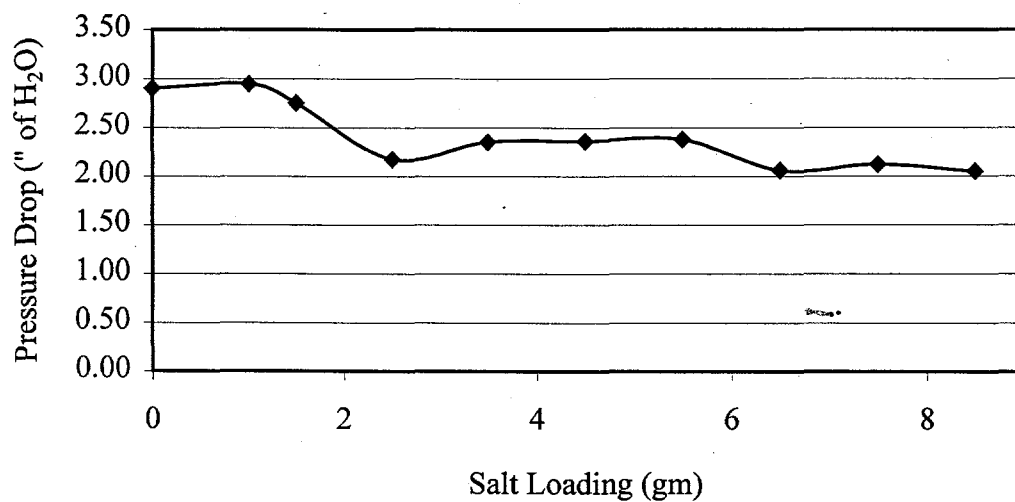


Figure B.16 Salt Loading Experiment with LiNO_3 for 350 grams of US Silica L-60 at 500°C.

B.4) Generation II – Data Collection Procedures/Results

The second generation fluidized bed reactor was designed to fluidize larger diameter particles in order to take advantage of the greater inertial forces present in the bed of particles. The larger particle diameters and greater superficial velocity through the bed will increase the Reynolds number and hopefully overcome the molten salt's viscosity and high surface tension. Potter's Glass Ballotini, which are >99% pure silica spheres, between 300-1100 microns were chosen for the initial experiments in the section. Table B.2 lists the potential samples of glass ballotini available for experimentation along with their advertised and experimentally determined average particle size range.

The particles were purchased from Potters Industries Inc. The experimentally determined particle size ranges were determined with Fisher Scientific USA Standard testing Sieves and a Cenco Sieve Shaker. A majority of the samples were well within the advertised size range. During the sieving process the fraction of the sample that did not reside on the main sieve tray was discarded. The remaining particles were discarded attempting to narrow the sample's particle size distribution and improve its fluidization characteristics.

The set up for the pressure drop measurement was altered for the generation II experiments to prevent clogging and give greater flexibility for measuring the pressure drop over different regions. A general schematic for the new pressure drop set up is shown in Figure B.6. The addition of the new tube into the bottom of the reactor made measuring the pressure drop over three different regions possible simply by manipulating the valves. Figure B.17 contains valve configurations for measuring the pressure drop across the bed of particles and the distributor plate (Configuration #1), pressure drop across the bed of particles (Configuration #2), and the pressure drop across the distributor plate (Configuration #3). In order to accommodate the higher flow rates encountered in this section of experiments, the pressures gauges were replaced with a (0-3.74E4) Pa (0-150)" of H₂O gauge for measuring the inlet reactor pressure and (0-1.25E4) Pa (0-50)" of H₂O gauge for measuring the pressure drop across the different regions of interest.

To minimize clogging in the pressure tube inserted into the bed of particles, configuration #4 was used anytime the reactor was heating up or the flow rate through the reactor was increased. This kept the pressure inside the tube higher than the pressure of the gas above the distributor plate. This method proved very effective in keeping the particles from clogging the pressure tube. During data collection for minimum fluidization and salt loading experiments, the pressure drop measurements using configuration #1 and #2 were recorded and continually compared to each other to ensure that the changes in the corresponding pressure drop measurements were consistent. This method would detect when the pressure tube was clogged and the pressure drop measurement across the bed of particles was no longer accurate.

Table B.2 Potters Glass Ballotini Particle Size Characteristics.

Sample Identification	Advertised Size Range (µm)	Particle Size Range (µm)	Sieve Size	Mass of Sample (grams)
1922 Lot 1117 (98)	150-250	212-300	70-50	758.81
		150-212	100-70	141.45
P-0120 Lot 1119	210-300	212-300	70-50	806.34
P-170 Lot 1 4/93	300-430	300-425	50-40	844.4
Mil #5 Lot 119 (98)	300-425	300-425	50-40	750.24
		425-600	40-30	106.1
B Lot 1119 (98)	425-600	425-600	40-30	891.9
A-055 Lot 073198	500-600	425-600	40-30	904.16
A-065 Lot 1 12/96	600-710	600-850	30-20	892.7
A Lot 1117 (98)	600-850	600-850	30-20	832.29
A-085 Lot 2 1/97	710-850	850-1180	20-16	882.89
A-90 Lot 120897	800-1100	850-1180	20-16	817.45
A-110 Lot 070798	1000-1200	850-1180	20-16	875.96

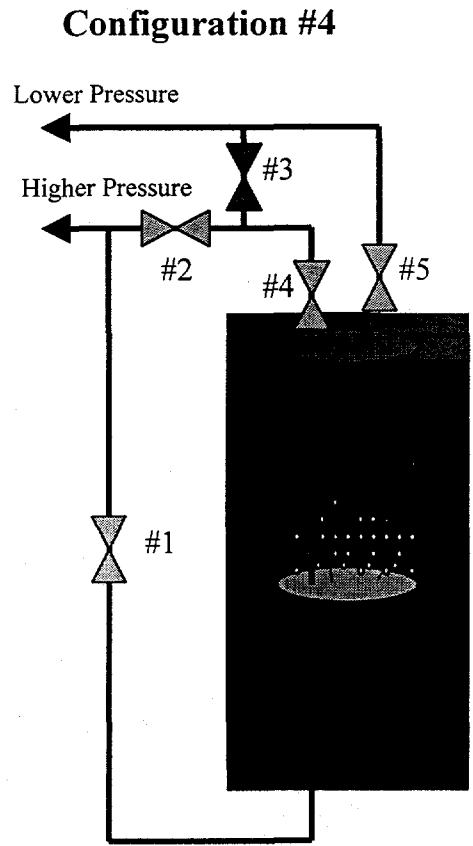
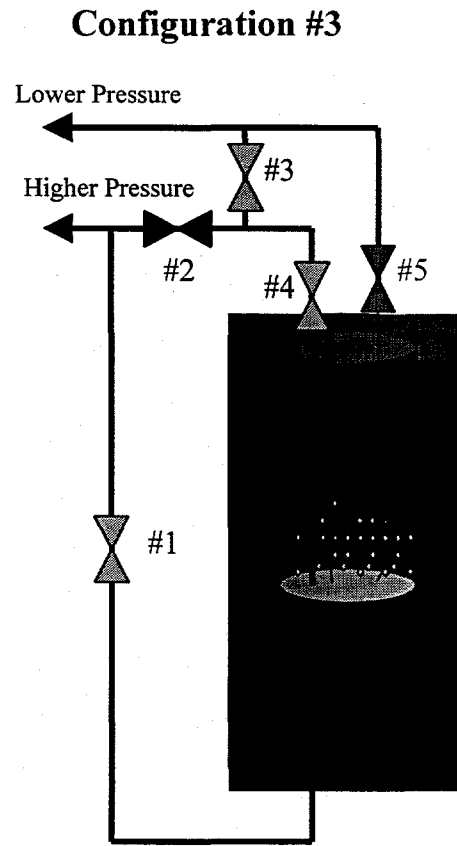
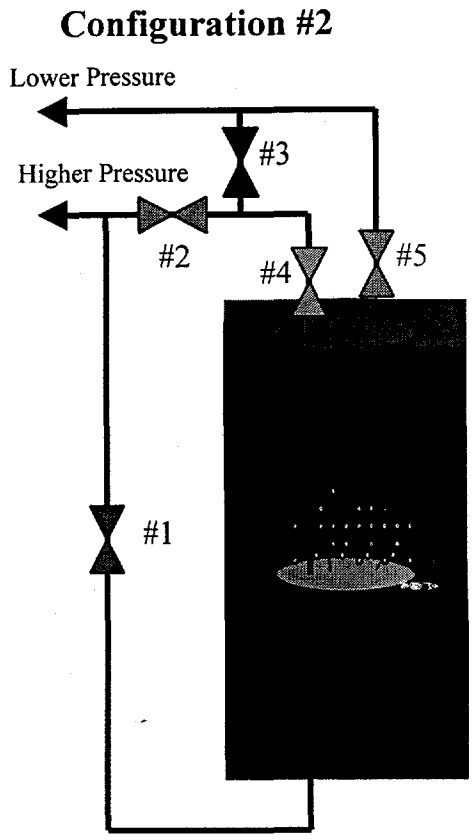
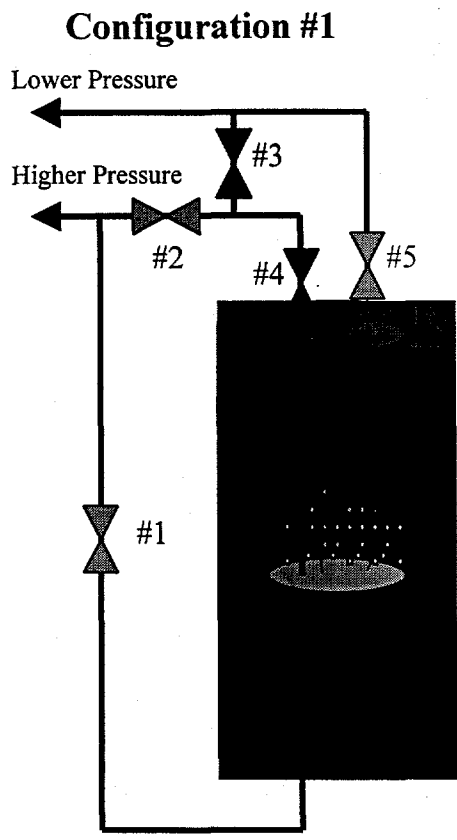
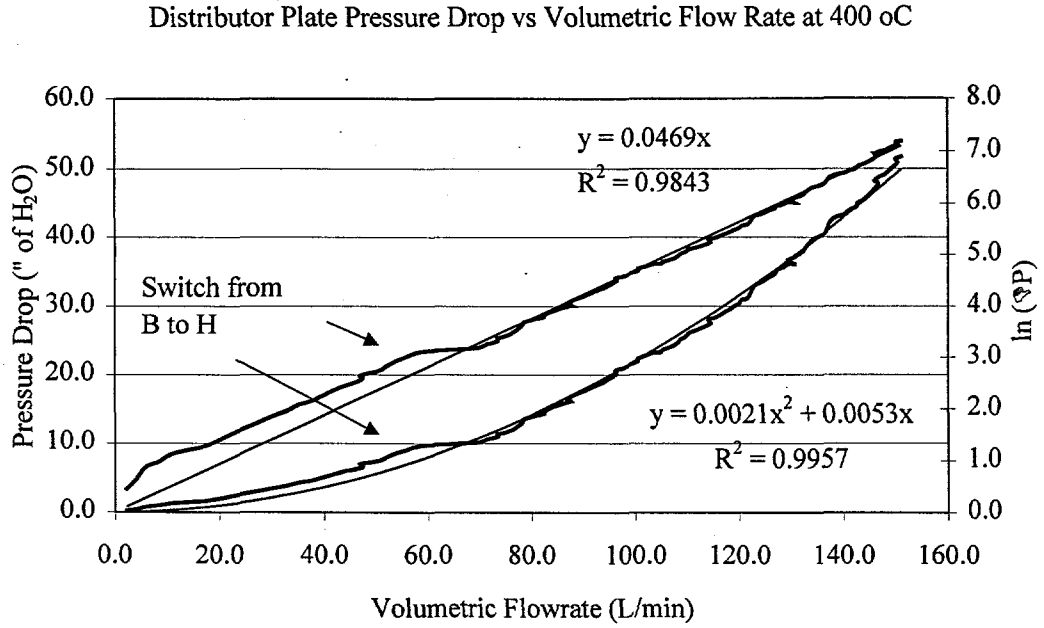


Figure B.17 Generation II Pressure Drop Measurement Configurations.

An attempt was made to develop a curve fit equation for the pressure drop across the distributor plate as a function of the volumetric flow rate and temperature as a backup to the pressure drop measuring system just described. The pressure drop across the distributor plate and the volumetric flow rate data were taken and then plotted for various temperatures. The orifice equation has the pressure drop proportional to the square of the volumetric flow rate ($\Delta P \propto Q^2$). Figure B.18 shows a sample of the data collected for the distributor plate pressure drop versus volumetric flow rate at 400°C. The expectation is for a straight line to form by plotting the square root of the pressure drop against the flow rate. Figure B.18 does give a plot very close to a straight line, but there is a sudden change in the line around 60 (L/min). This discontinuity occurs when switching from the B to H flowmeter. There is a slight difference between the distributor plate pressure drop for the same "measured" flow rate between the two flowmeters. After extensive discussions with the support staff at Brooks Instruments, the validity of the temperature and pressure corrections made to calculate the actual flow rates were verified. It was concluded that the B flowmeter is not as accurate at the lower region of its scale and at pressures significantly lower than its calibrated pressure 3.4E4 Pa (5 psig). Even small differences between the two flowmeters can make a big difference at elevated temperatures. The reactor temperature correction exacerbates the error and makes developing one equation for the distributor plate pressure drop as a function of volumetric flow rate impractical.

Figure B.18 Generation II Distributor Plate Pressure Drop versus Volumetric Flow Rate at 400°C.



B.4a) Minimum Fluidization Calculations for "P-170"

The glass ballotini support "P-170" was chosen to test out the new fluidized bed reactor and pressure drop measuring system. The first experiments compared the experimental pressure drop above minimum fluidization to the theoretical value to test the new reactor. For a particle loading of 350 grams and bed diameter of 7.49 cm (2.95"), the pressure drop across the bed of particles bed loading should be just over 7.47 Pa (3" of H₂O). Figures B.19-B.22 are all minimum fluidization curves for "P-170" at four different temperatures. The experiments began by loading the particles into the reactor with sufficient flow through the bed to keep the particles from falling through the distributor plate. The reactor was then brought up to temperature with the pressure drop measuring system in configuration #4. Once the desired temperature was reached, the pressure drop readings were taken for both configurations #1 and #2 along with the inlet pressure from Validyne PTDR #.2 The graphite element temperature was also lowered as the flow rate was decreased through the bed to maintain the reactor temperature to within +/- 5 °C of the desired reactor temperature. The minimum fluidization figures show that an average measured pressure drop above the minimum fluidization point is typically around 747 Pa (3.0" of H₂O), which matches extremely well with the theoretical value. There was excellent dynamic response in the pressure drop measurements along with a clear pressure tube upon cleaning the reactor. These facts point toward the improved accuracy and effectiveness of the new pressure drop measuring system.

The minimum fluidization velocities at elevated temperature were significantly lower than at ambient temperature, which concurs with theory. The minimum fluidization velocity at ambient temperature is around 8.0 cm/s.

B.4b) Trial Salt Loading Experiments

Three salt loading experiments were completed to test out the salt feeder at higher gas velocities through the reactor and to see how the pressure tube responded to the presence of molten salt. The salt loading experiments were run at 300°C at $4u_{mf}$, then 500°C at $5u_{mf}$ and finally at 500°C at $7.5u_{mf}$ to examine the pressure drop behavior. For the first trial, LiNO₃ was injected using the pneumatic salt feeder at one-gram increments. Prior to using the salt feeder to inject salt into the reactor, two "dry" injections were performed to examine the bed's response to a blast of high-pressure nitrogen. The nitrogen without the salt had no sustained effect on the pressure drop across the bed.

Minimum Fluidization Curve: Pressure Drop vs Superficial Velocity (Temp 25°C, Support 350 gm of Glass Ballotini "P-170")

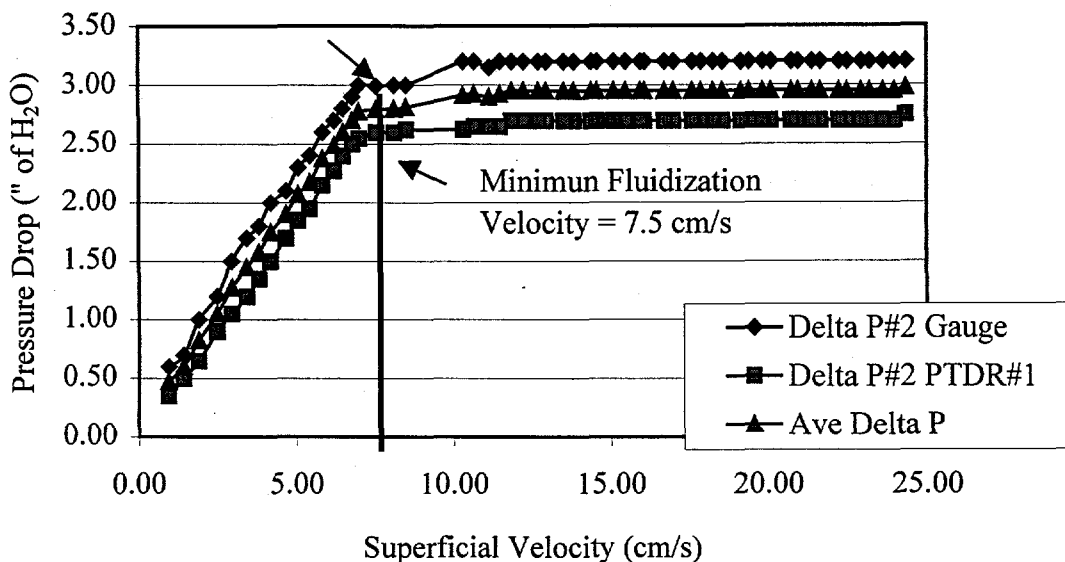


Figure B.19 Minimum Fluidization Curve for 350 grams of Glass Ballotini "P-170" at 25°C.

Minimum Fluidization Curve: Pressure Drop vs Superficial Velocity (Temp 300oC Support 350 gm of Glass Ballotini "P-170")

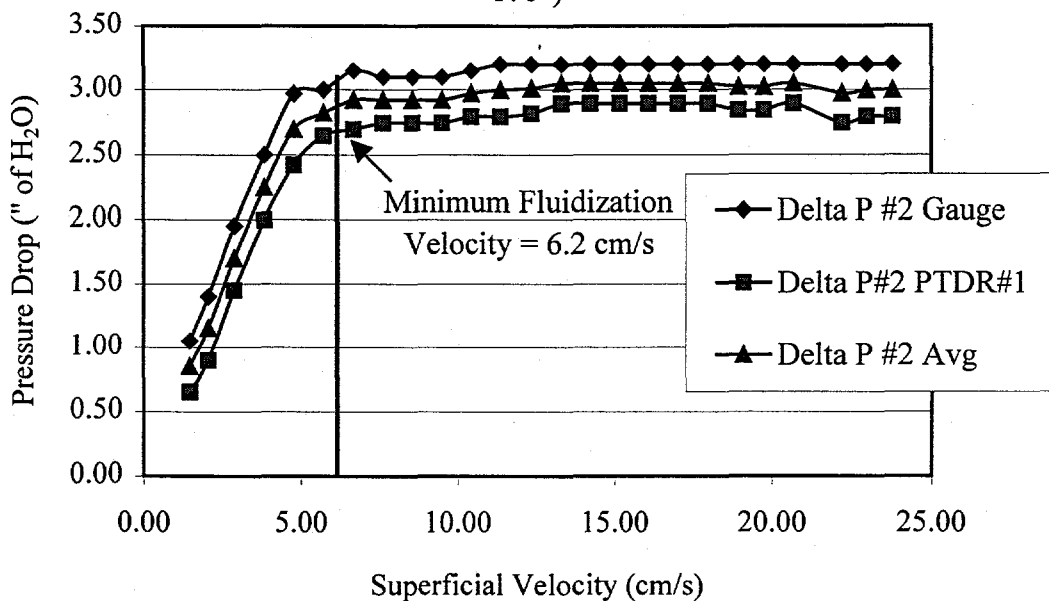


Figure B.20 Minimum Fluidization Curve for 350 grams of Glass Ballotini "P-170" at 300°C.

Minimum Fluidization Curve: Pressure Drop vs Superficial Velocity (Temp 400oC Support 350 gm of Glass Ballotini "P-170")

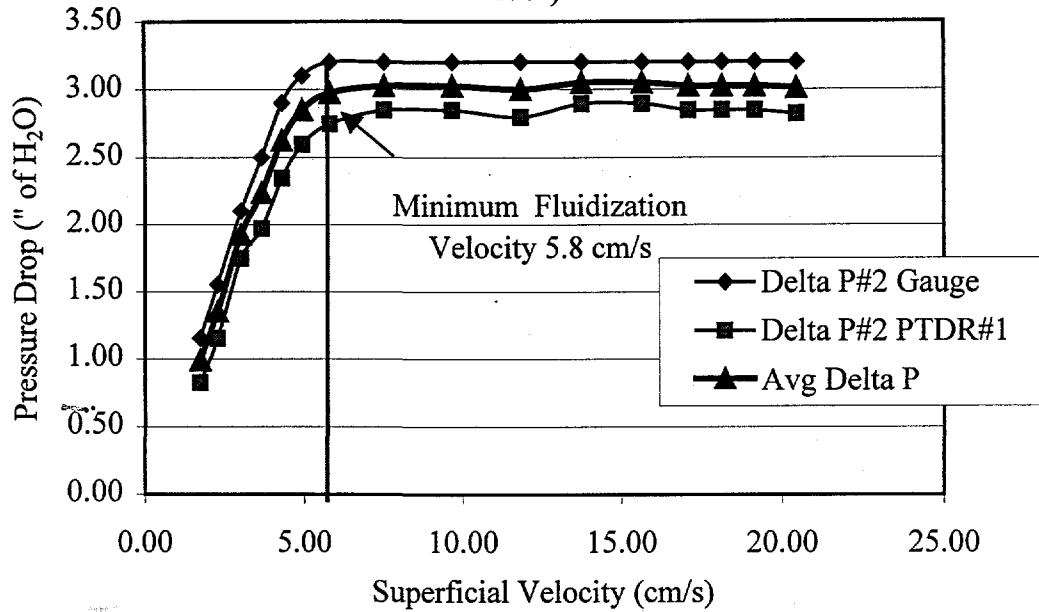


Figure B.21 Minimum Fluidization Curve for 350 grams of Glass Ballotini "P-170" at 400°C.

Minimum Fluidization Curve: Pressure Drop vs Superficial Velocity (Temp 500oC Support 350 gm of Glass Ballotini "P-170")

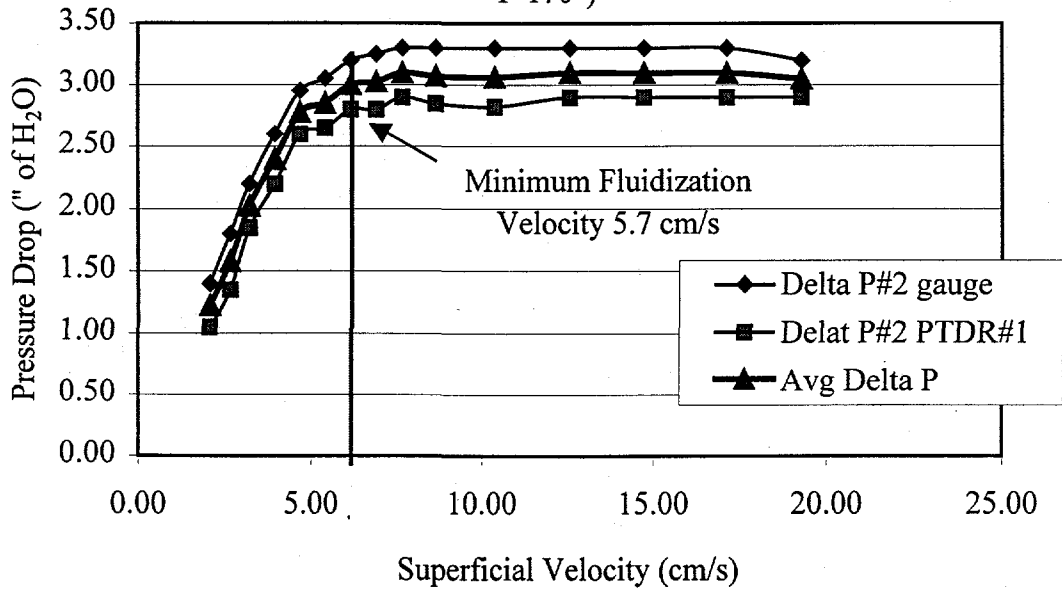
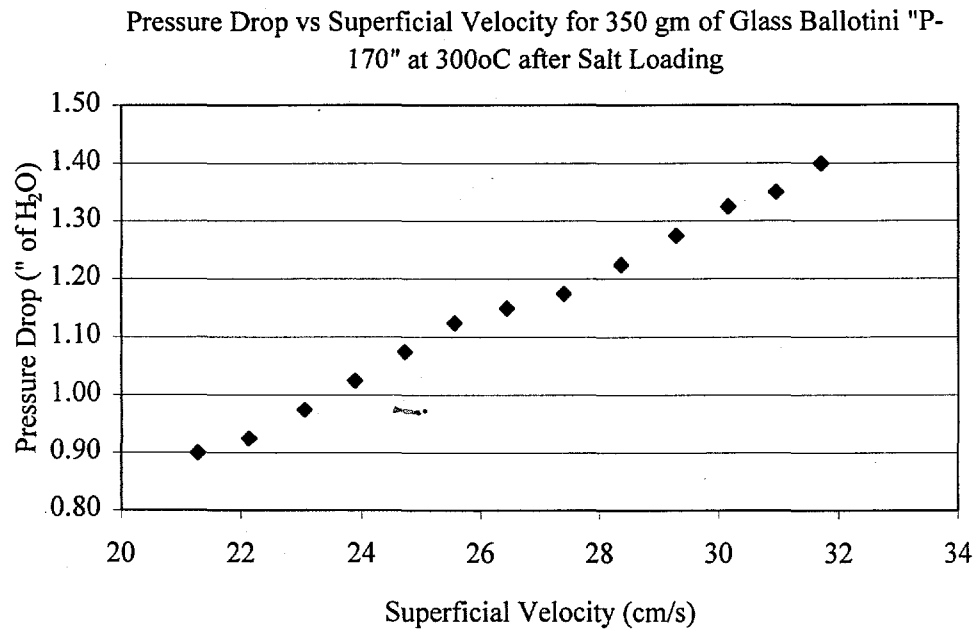


Figure B.22 Minimum Fluidization Curve for 350 grams of Glass Ballotini "P-170" at 500°C.

While fluidized at 300°C and $4u_{mf}$, salt was added to the reactor. The first gram of salt caused the bed to collapse, which was signified by a dramatic decrease in the pressure drop across the bed and a slight temperature drop in this case. Five more grams of salt were injected over a period of 12 hours, but the pressure drop never recovered. The final pressure drop across the bed was 224 Pa (0.9" of H₂O). Prior to cooling the reactor, the volumetric flow rate through the bed was increased to determine its effect on the pressure drop. If the bed was still in a fluidized state, the pressure drop should stay approximately constant while increasing flow rate. Figure B.23 shows that a linear relationship between the pressure drop and the superficial velocity exists, which indicates a collapsed bed. A solid matrix of particles and salt that had formed on top of the collapsed bed was visible upon taking the reactor apart. The matrix was easily broken up with a metal rod and the bed refluidized at ambient temperature. The particles were removed using a vacuum and then ground with a mortar and pestle to break up the remaining agglomerates.

Figure B.23 Linear Relationship between ΔP and Volumetric Flow Rate across a Collapsed Bed.



An additional five grams of LiNO_3 were added to the particles before putting them back into the reactor. The particles were easily fluidized at ambient temperature. This experiment looked to see if there was any difference in the bed behavior when the salt is already present in the fluidized bed as the salt melts. The pressure drop was recorded every 20°C as the reactor temperature increased. The pressure drop remained constant up to 250°C , which happens to be the melting point of LiNO_3 . The pressure drop decreased only slightly as the temperature continued to go up until reaching 270°C . The temperature paused for almost five minutes during which the pressure drop went down significantly. The pressure drop continued to decrease as the temperature went up, presumably due to the bed of particles collapsing.

The next experiment, at 500°C at $5u_{mf}$, exhibited some very bizarre behavior. The first attempt at this experiment saw the bed collapse as the reactor heated up. Again, the bed collapse occurred at a temperature slightly higher than LiNO_3 's melting point. The Inconel™ reactor at the end of the previous experiment was only cleaned with a vacuum to remove the clumps of particles and salt and the a wire brush and damp sponge to remove the remaining salt on the reactor walls. Apparently, the small amount of salt that was still on the walls of the reactor was enough to initiate bed collapse. This meant that after each experiment the entire fluidized bed had to be removed and water washed before the addition of new, clean particles.

The reactor was removed and new particles were added. The water washing worked as the pressure drop remained constant while passing through the salt's melting point. With a reactor temperature of 500°C at $5u_{mf}$ there was an average pressure drop of 747 Pa ($3.0''$ of H_2O) across the fluidized bed. The salt feeder was "dry" injected twice with no effect. Initially, 0.25 grams of salt were injected into the bed with no effect on the pressure drop. Then another 0.25 grams was injected and the bed collapsed as indicated by a sharp decrease in the bed temperature and pressure drop. Over a period of two hours the temperature climbed up to just below the original value, as did the pressure drop. This same phenomenon was observed after each successive addition of 0.25 grams of salt, with the exception that the temperature did not return to 500°C unless the graphite element temperature was increased. On the first two occasions, as the bed refluidized the temperature in the reactor jumped all the way up to 550°C . This occurred because the graphite element temperature was increased to warm the bed back to the original temperature of 500°C , not expecting the bed to refluidize. The temperature jumped quickly when the bed refluidized. The bed appeared to refluidize with each successive addition of salt, up to 6.25 grams.

The collapsed bed at ambient temperature looked similar to the previous experiment, but it had a distinct green color to it. It was also very difficult to break up, and the agglomerates no longer dissolved during water washing. Considering all of these factors it appears that a chemical reaction occurred, which might somehow attribute to this bizarre refluidization phenomenon. Not once in the remaining salt loading experiments performed did the bed refluidize once it had collapsed.

This experiment was repeated to see if the results could be duplicated. In this case, after salt addition, the bed collapsed and never refluidized even after waiting for

over 24 hours. The apparent chemical reaction occurred again indicating that once should avoid this temperature in the future.

B.4c) Glass Ballotini Experimental Design

To efficiently investigate the various glass ballotini supports, an experimental design matrix was created as seen in Figure B.24. The variables of interest are temperature, velocity above minimum fluidization, and particle size. The experiments were all run at 400°C. The temperature was fixed at 400°C in order to avoid the apparent chemical reaction around 500°C and temperatures in the bed below the melting point if operated around 300°C due to large radial temperature developing gradients upon bed collapse.

Four different average diameter supports covering the 300-1100 micron size range were selected for the experimental design matrix in Figure B.24. The four supports chosen are listed in Table B.3.

Table B.3 Glass Ballotini Specs for Experimental Design Matrix.

Designator	Avg dp (Microns)
MIL #5 Lot 1119	350
A-055	550
A-085	850
A-110	1100

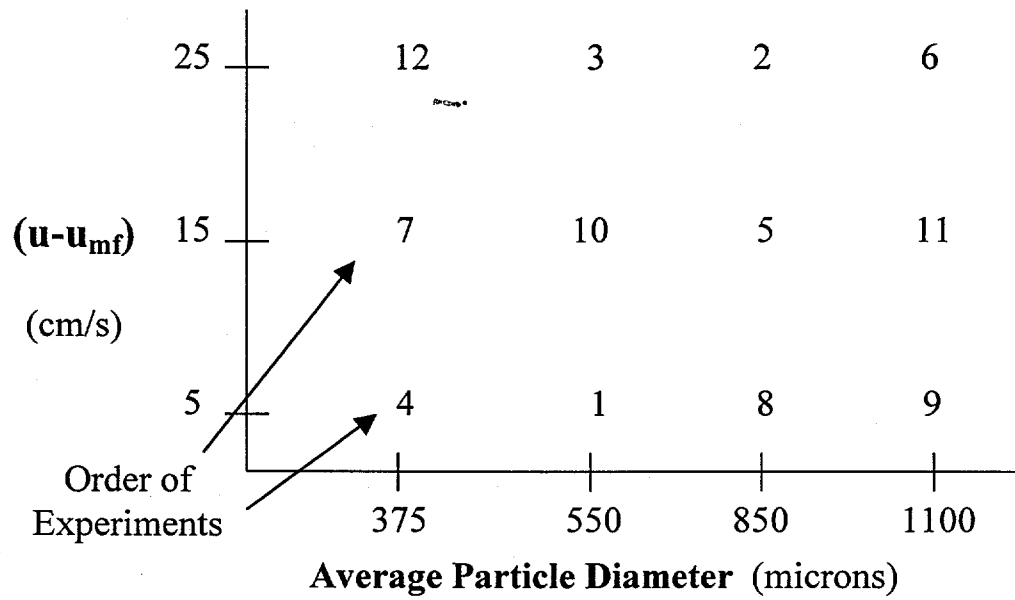


Figure B.24 Glass Ballotini (375-1100 μm) with the Pneumatic Salt Injector Experimental Design Matrix.

Drawing numbers out of a hat randomized the order of experiments. Prior to running the salt experiments, the minimum fluidization curves for each support were generated. Figures B.25-B.28 contain the minimum fluidization curves for the supports tested in this section. The fluidization curves' pressure drops above the minimum fluidization velocity are consistent from support to support and match well with the theoretical values. The minimum fluidization velocities are also consistent with theoretical predictions. The individual support's minimum fluidization velocities at 400°C are all lower than those predicted by theory at ambient temperature.

Minimum Fluidization Curve: Pressure Drop vs. Superficial Velocity (Temp 400oC Support 350 gm of Glass Ballotini "MIL #5 Lot 1119")

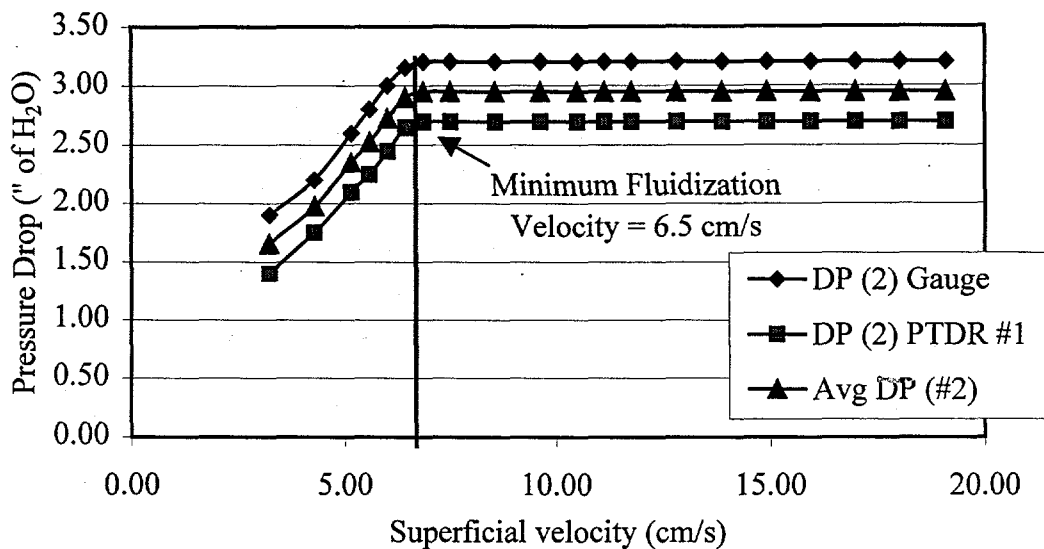


Figure B.25 Minimum Fluidization Curve for 350 grams of Glass Ballotini MIL #5 Lot 1119 at 400°C.

Minimum Fluidization Curve: Pressure Drop vs Superficial Velocity (Temp 400oC Support 350 gm of Glass Ballotini 'A-055')

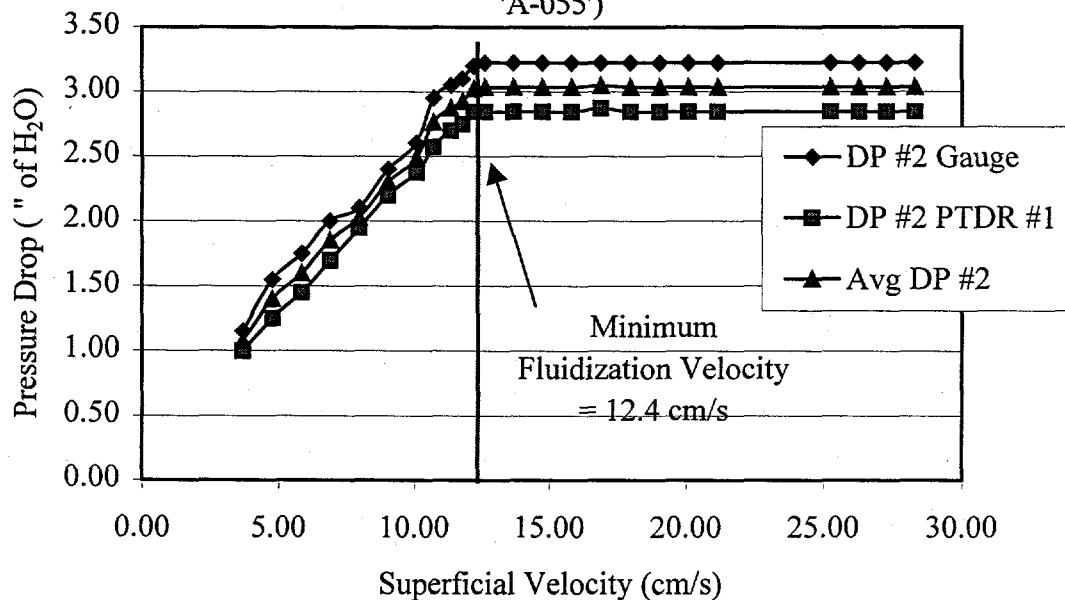


Figure B.26 Minimum Fluidization Curve for 350 grams of Glass Ballotini "A-055" at 400°C.

Minimum Fluidization Curve: Pressure Drop vs. Superficial Velocity (Temp 400oC Support 350 gm of Glass Ballotini "A-085")

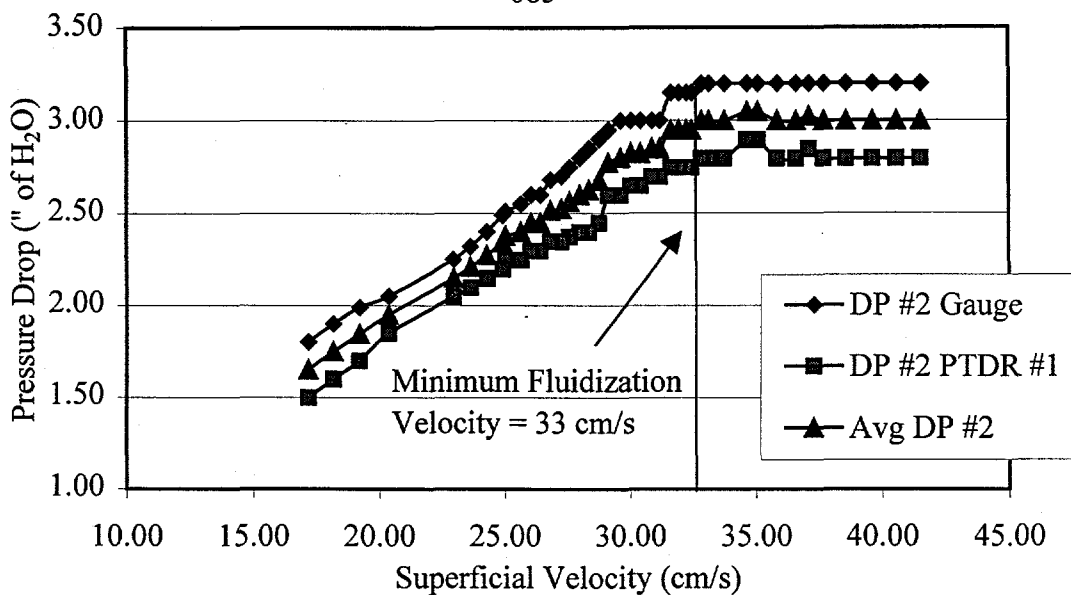
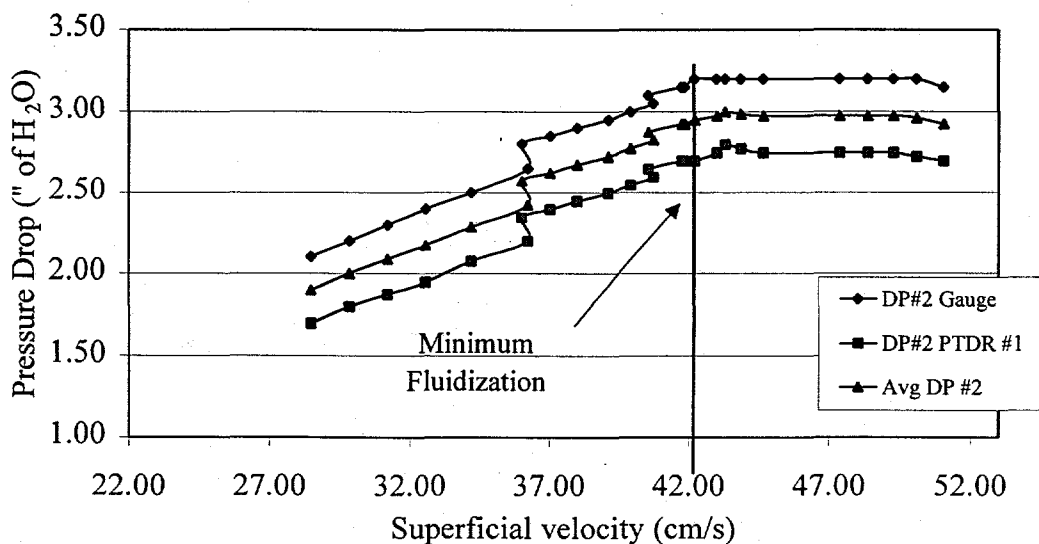


Figure B.27 Minimum Fluidization Curve for 350 grams of Glass Ballotini "A-085" at 400°C.

Figure B.28 Minimum Fluidization Curve for 350 grams of Glass Ballotini "A-110" at 400°C.

Minimum Fluidization Curve: Pressure Drop vs. Superficial Velocity (Temp 400oC Support 350 gm of Glass Ballotini, "A-110")



Salt was injected into the fluidized bed at either 0.25 or 0.5 gram increments. The amount of salt injected did not change the fluidization characteristics of the bed from one experiment to another. In all cases, the bed had collapsed after adding a total of 1.5 grams of LiNO_3 , and in many cases the bed collapsed immediately after adding the first 0.25 or 0.5 grams. The results of this section, seen in Table B.4, do not shed a favorable light on the potential for high temperature fluidization for non-porous glass spheres in the presence of molten salts.

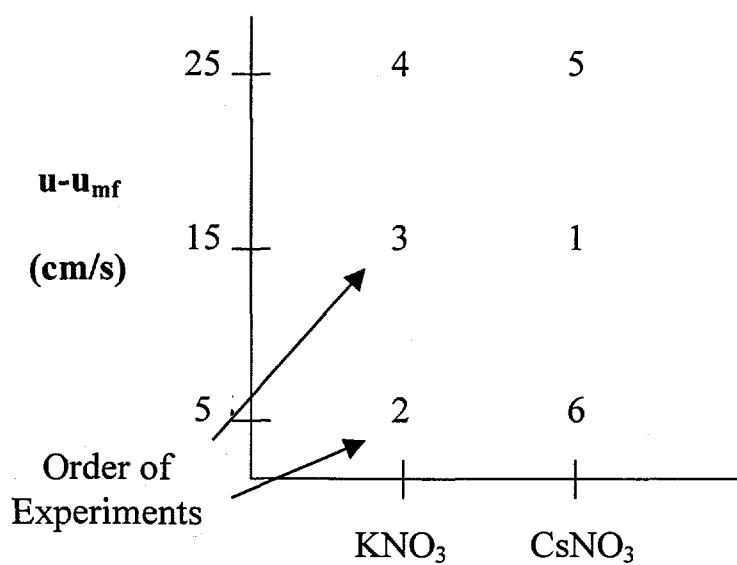
B.4d) Zirconia Experimental Design Matrix

The next set of experiments was performed to see if changing the type of support (the density) and the type of salt (surface tension) affected the bed's ability to stay fluidized. The support consisted of 300 micron, spherical, non-porous zirconia particles generously donated by the TOSOH Company. KNO_3 and CsNO_3 were the salts for this set of experiments. KNO_3 and CsNO_3 both have higher melting points than LiNO_3 , around 350°C and 401°C , respectively. This is the reason the higher temperature, 500°C , for this simple experimental design matrix was chosen. The experimental design matrix for this set of experiments is shown in Figure B.29. The minimum fluidization curve for the zirconia particles at 500°C is found in Figure B.30. Due to the higher density of the zirconia particles, a 450 gram bed mass was used in order to have a sufficient bed height to achieve uniform fluidization.

Table B.4 Amount of Salt Injected (grams) Causing SiO₂ Fluidized Bed to Collapse.

$(u-u_{mf})$ cm/s	Support			
	MIL #5 Lot 1119	A-055	A-085	A-110
5	(0-0.5)	(0-0.5)	(0-0.5)	(0.5-1.0)
15	(0-0.5)	(0.5-1.0)	(0-0.5)	(1.0-1.5)
25	(0-0.5)	(0-0.5)	(0.5-1.0)	(0-0.5)

Figure B.29 TOSOH Zirconia Spheres (300 μ m) Experimental Design Matrix.



Theory predicts a pressure drop of 968 Pa (3.89" of H₂O) across the bed above the minimum fluidization point. The experimental pressure drop above minimum fluidization is only around 846 Pa (3.4" of H₂O). Since ZrO₂'s density is 2.5 times that of SiO₂, the pressure drop occurs over a much shorter distance in the vertical direction. The pressure tube that measures the pressure directly above the distributor plate has holes drilled in the end of the tube. These holes do not start immediately above the distributor plate. The holes are in fact almost 2 mm above the distributor plate due to having the drill above the plug in the end of stainless steel tube. This artifact of the experimental apparatus did not have as pronounced an effect when using the SiO₂ particles due to its lower density. The second reason for the lower pressure drop value stems from the small amount of ZrO₂ support available for experimentation. Without a sufficient bed height, the gas does not get evenly distributed through the particles and part of the bed does not fluidize. These two reasons are proposed for the observed lower pressure drop. The experiments in Figure B.29 were still run, in light of this disparity. The result of these experiments was similar to the previous section. All but one of the experiments saw the bed collapse shortly after adding the first 0.5 grams of salt. Table B.6 contains the amount of salt added to the reactor prior to the bed collapsing. Bed collapse was assumed when a temperature decrease and sharp decline in the pressure drop across the bed of particles was observed. Again, fluidization in the presence of molten salts for this region of parameter space with non-porous particles does not appear feasible.

Figure B.30 Minimum Fluidization Velocity for 450 grams of TOSOH Zirconia at 500°C.

Minimum Fluidization Curve: Pressure Drop vs. Superficial Velocity
(Temp 500oC Support 450 gm off TOSOH ZrO₂, 300 micron)

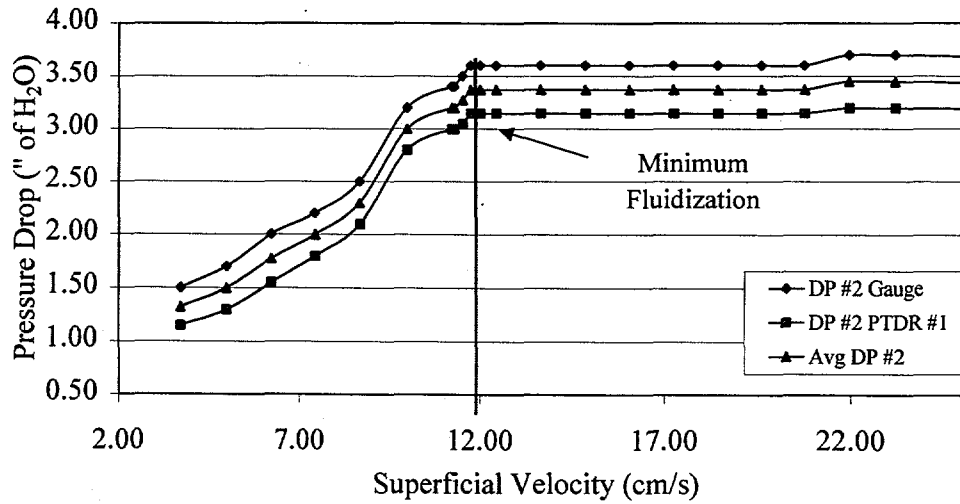


Table B.5 Amount of Salt Injected (grams) Causing ZrO₂ Fluidized Bed to Collapse.

(u-u _{mf}) cm/s	Salt	
	KNO ₃	CsNO ₃
5	(0.5-1.0)	(0-0.5)
15	(0-0.5)	(0-0.5)
25	(0-0.5)	(0-0.5)

B.4e) Aqueous Salt Syringe Injector Experiments

This set of experiments was completed using the silica particles listed in Table B.2. The experimental design matrix in Figure B.24 was run again with the same procedures except for the method of salt injection. A saturated solution of LiNO_3 was made. At room temperature, roughly 90 grams of LiNO_3 is soluble in 1 Liter of water. 5 mL of salt solution was injected into the fluidized bed reactor. 5 mL of solution contains approximately 0.45 grams of salt. Water without salt present was injected into the fluidized bed prior to each run to act as a control. In each case, the water did not change the pressure drop across the bed. The temperature in the bed naturally decreased upon injection of the water, but within a couple of minutes it would return to its original value. Only eight of the twelve experiments were completed in the experimental design matrix. The different method of injection did not produce tangible differences from the previous experiments. Table B.8 lists the total amount of salt injected that caused the bed to collapse.

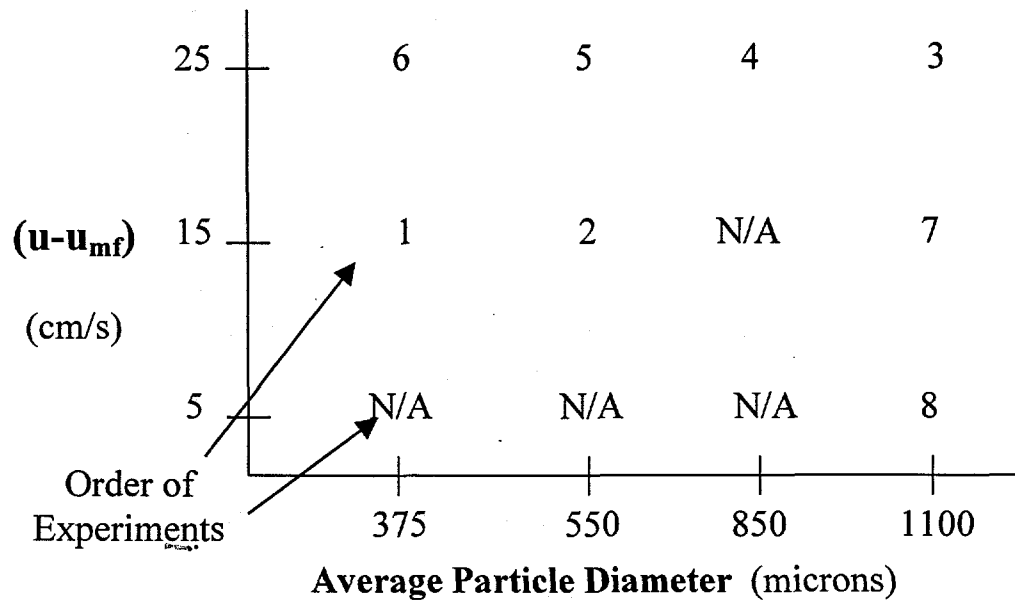


Figure B.31 Glass Ballotini (375-1100 μm) with Aqueous Salt Injector Experimental Design Matrix.

Table B.6 Amount of Salt injected (grams) causing SiO_2 Fluidized Bed to Collapse Using an Aqueous Syringe Injector.

$(u-u_{mf})$ cm/s	Support			
	MIL #5 Lot 1119	A-055	A-085	A-110
5	(0-0.45)	(0.9-1.35)	(0.45-0.9)	(0.45-0.9)
15	(0-0.25)	(0-0.45)	N/A	(0.9-1.35)
25	N/A	N/A	N/A	(0-0.45)